Western University
Faculty of Engineering

Department of Mechanical and Material Engineering

Project Report MME 9614A

"Applied Computational Fluid Mechanics and Heat transfer"

"Numerical Study on Effects of Near Wall Treatment on the Hydrodynamics of Circulating Fluidized bed and Validation with Experimental Results"

Course Instructor- Prof. Chao Zhang

Submitted By:

Jagdeep Singh

Student No. 250911825

December, 2016

Chapter 1. Problem Description:

This project involves the study of effects of near wall treatment on the hydrodynamics of CFB. The simulation was carried out in Fluent 16.2 on 2D- Mesh which generated in ICEM based on $Y^+ \sim 1$. Furthermore, the numerical results are validated against the experimental data. The general arrangement of the Riser is shown in Fig. (1).

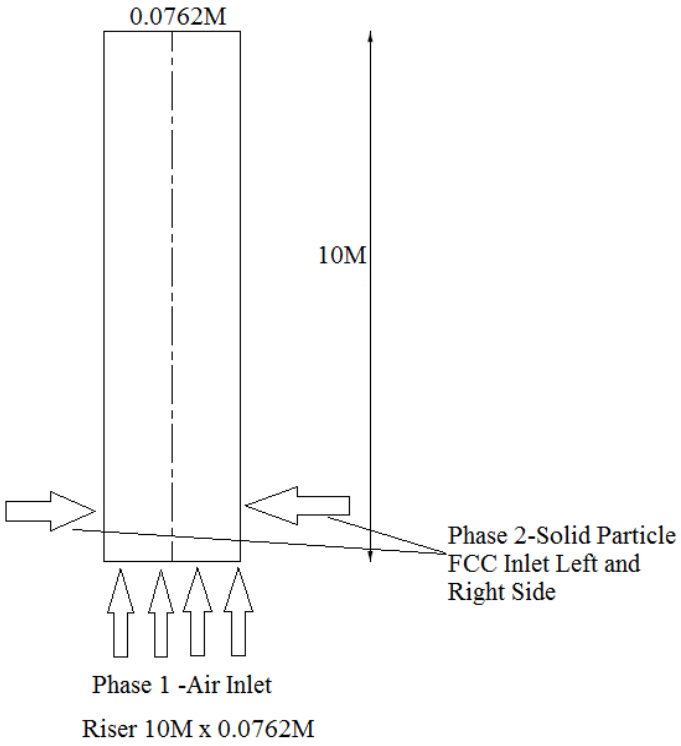

Fig. (1) General Arrangement of the Riser

1.2 Operating Conditions

Table 1. Operating conditions

Properties	**Values**
Solid Particle(FCC) Density	1500 kg/m^3
Circulation Rate of Solid Particle	100 kg/m^{2}s
Superficial Gas velocity	5 m/s
Packing Limit	0.63
Specularity Coefficient	0.0001
Restitution Coefficient	0.95

1.3 Introduction

In a vertical column, the solid particles are maintained at the static height and gas is blown from the bottom then solid particle behaves like a fluid. This phenomenon is called fluidization. The superficial gas velocity that is required to start this process is called minimum fluidization. When the gas velocity is further increased, it crosses the terminal velocity then circulation of solid particle starts. The circulating fluidized bed comprises of Riser and Downer. All the chemical reactions and processes are take place in the riser and downer is used to collect the entrained particles and feed them again to riser part therefore a circulation of solid particle can be considered. The main component of circulating fluidized bed is Riser. Therefore, this project involves the 2D CFD study of effects of near wall treatment on the hydrodynamics of the circulating Fluidized bed and Furthermore, the numerical investigation is then compared with the experimental studies for validation process. The circulating Fluidized bed found its application in Chemical, Petrochemical, Energy sector and Environmental engineering due to its characteristics of gas-particle and particle-particle mixing.

1.4 Flow regimes in fluidization

There are number flow regimes that exists before fluidization occurs. Initially, when the solid bed is at static height it is called fixed bed as shown in Fig. (2) as the velocity of the gas increases further solid particle rise creating voids. In further increase in gas velocity the suspension of particle increases in the gas this is called slugging regime and after this turbulent regime is obtained with the increase in velocity. The last regime is known as fast fluidization because in this regime almost all the particle got suspended in the air.

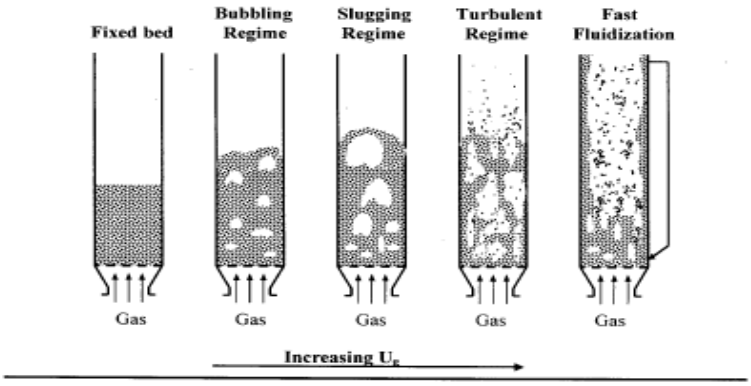

Fig. 2.1: Fluidization regimes.

[1]Fig. (2) Flow Regimes in fluidization

[1] CFD modelling of the hydrodynamics of circulating fluidized bed by Adnan M. AMUTTAHAR

1.5 Goals:

1) The objective of this project is to study the near wall treatment on the hydrodynamic properties of the circulating fluidized bed.

2) Simulation was done on 2D-CFD model of circulating fluidized bed.

3) Three different wall functions were compared namely standard, scalable and Menter Lechner model.

4) comparison of solid holdup and particle velocity with experimental data.

Chapter 2: Mathematical Modelling

To model a circulating fluidized bed mathematically, we choose 2D CFD model to minimize computational domain and time. From the physical aspect of circulating fluidized bed our interest is to study effects of near wall treatment on the hydrodynamic properties of CFB only in riser. The two-phase unsteady flow is modeled as Eulerian-Eulerian granular flow. In this model, the particle wall interaction and particle-particle interaction is taken into account by choosing the specularity coefficient and solid pressure. In dilute flow, the consideration of continuum hypothesis is valid for both the gas and solid phase. Therefore, the continuity and momentum equation for both the solid and gas phase will be solved.

2.1 **Continuity Equation:**

$$\frac{\partial}{\partial t}\left(\alpha_q \rho_q\right) + \nabla.\left(\alpha_q \rho_q \overrightarrow{v_q}\right) = \sum_{q=1}^{n}(\dot{m}_{pq} - \dot{m}_{qp}) + S_q \qquad \text{Eq. (1)}$$

Where;

α_q is the volume fraction for phase q

$\overrightarrow{v_q}$ is the velocity of phase q

$\dot{m}_{pq}$ is the mass transfer from p to q phase

$\dot{m}_{qp}$ is the mass transfer from q to p phase

2.2 **Momentum Equation:**

$$\frac{\partial}{\partial t}\left(\alpha_q \rho_q \overrightarrow{v_q}\right) + \nabla.\left(\alpha_q \rho_q \overrightarrow{v_q}\overrightarrow{v_q}\right) = -\alpha_q \nabla P_q + \nabla.\left(\alpha_q \tau_q\right) + \alpha_q \rho_q \vec{g} + m_q \qquad \text{Eq. (2)}$$

Where;

τ_q is the second order reynold stress tensor which is explained in turbulent model in the later section

2.3 **Granular Model:**

In this numerical simulation, the granular model has been used to simulate particle-wall interaction and particle-particle interaction. For the closure of solid phase momentum equation, effective stresses of solid phase must be defined. Effective stresses for the solid can be calculated with an analogy of kinetic theory of gases. These stresses originate from particle-particle and wall-particle interaction. To model the granular flow, the kinetic theory of gases has been used. Therefore, the granular temperature is defined for solid particle in a similar manner as temperature of gases is

defined in Kinetic theory of gases. The magnitude of particle fluctuation is called the granular temperature. This concept is described by Lun et al. (1984). The granular temperature equation is given below which is used in Fluent solver. In this numerical simulation, Partial differential model for granular temperature is selected and different model has been selected to model other properties such as granular viscosity model, granular bulk viscosity model, granular conductivity, solid pressure, radial distribution, elastic model and these are represented in the below section:

Granular equation:

$$\frac{3}{2}\left[\frac{\partial}{\partial t}(\rho_s \alpha_s \Theta_s) + \nabla.(\rho_s \alpha_s \vec{v}_s \Theta_s)\right] = (-p_s \bar{I} + \bar{\tau}_s): \nabla \vec{v}_s + \nabla.(k_{\Theta s} \nabla \Theta_s) - \gamma_{\Theta s} + \varphi_{is} \quad \text{Eq. (3)}$$

The granular temperature is defined as the fluctuating velocity components of the solid particles and is given below:

$$\Theta_s = \frac{1}{3} u_{s,i} u_{s,i} \quad \text{Eq. (4)}$$

Where;

$(-\mathrm{p_s}\bar{\mathrm{I}} + \bar{\tau}_\mathrm{s}): \nabla \vec{\mathrm{v}}_\mathrm{s}$ is the energy generation term by the solid stress tensor

$\mathrm{k_{\Theta s}} \nabla \Theta_\mathrm{s}$ is the diffusion term of energy

$\gamma_{\Theta \mathrm{s}}$ is the dissipation of energy by collision of particles

φ_{is} is the energy exchange between the ith phase of gas with sth phase of solid

The Syamlal Diffusion coefficient is given by the following Equation:

Granular conductivity: Syamlal et al. model is used for this numerical schemes for capturing the granular conductivity:

$$k_{\Theta s} = \frac{15 d_s \rho_s \alpha_s \sqrt{\Theta_s \pi}}{4(41-33\eta)} \left[1 + \frac{12}{5}\eta^2(4\eta - 3)\alpha_s g_{0,ss} + \frac{16}{15\pi}(41 - 33\eta)\eta \alpha_s g_{0,ss}\right] \quad \text{Eq. (5)}$$

Where,

$$\eta = \frac{1}{2}[1 + e_{ss}]$$

The Eq. (6) below gives the dissipation of energy due to collision of particles.

$$\gamma_{\Theta s} = \frac{12(1-e_{ss}^2) g_{0,ss}}{d_s \sqrt{\pi}} \rho_s {\alpha_s}^2 \Theta_s^{\frac{3}{2}} \quad \text{Eq. (6)}$$

The Eq. (7) predicts the energy transport between the i^{th} phase of the gas and s^{th} phase of the solid particle

$$\varphi_{is} = -3 K_{is} \Theta_s \quad \text{Eq. (7)}$$

The shear force at the wall is represented by the following Eq. (8) model

$$\vec{\tau}_s = -\frac{\pi}{6}\sqrt{3}\emptyset\frac{\alpha_s}{\alpha_{s,max}}\rho_s g_0\sqrt{\Theta_s}\vec{U}_{s,II} \quad \text{Eq. (8)}$$

$\vec{U}_{s,II}$ in the Eq. (8)represents the slip velocity along the wall

$\emptyset$ in the Eq. (8)represents the specularity coefficient

To capture the particle-wall interaction. The specularity must be defined for the wall boundary condition for the solid phase. In this numerical simulation, A specularity coefficient of 0.0001 used.

The Eq. (9) represents the general equation for the granular temperature:

$$q_s = \frac{\pi}{6}\sqrt{3}\emptyset\frac{\alpha_s}{\alpha_{s,max}}\rho_s g_0\sqrt{\Theta_s}\vec{U}_{s,II}.\vec{U}_{s,II} - \frac{\pi}{4}\sqrt{3}\frac{\alpha_s}{\alpha_{s,max}}(1-e^2{}_{sw})\rho_s g_0\Theta^{\frac{3}{2}}{}_s \quad \text{Eq. (9)}$$

The above equation is the general form of granular temperature derived using Eq. (4) to Eq. (9)

2.3.1 Granular viscosity model:

The granular viscosity is originated from collision viscosity and kinetic viscosity due to kinetic transport and collision transport. In this numerical study of circulating fluidized bed, Syamlal-O-Brien model is used. Therefore, granular viscosity model can be represented below:

Total Granular viscosity is represented in the Eq. (10)

$$\mu_s = \mu_{s,coll} + \mu_{s,kin} \quad \text{Eq. (10)}$$

Gidaspow and Syamlal o brien predicts the model represented in Eq. (11) for collision transport

$$\mu_{s,coll} = \frac{8}{5}\alpha_s\rho_s d_s g_0\eta\left(\frac{\Theta_s}{\pi}\right)^{1/2} \quad \text{Eq. (11)}$$

Syamlal o brien gave the Eq. (12) for viscosity due to kinetic transport:

$$\mu_{s,kin} = \frac{\alpha_s\rho_s d_s(\Theta_s\pi)^{1/2}}{12(12-\eta)}\left[1+\frac{8}{5}\eta(3\eta-2)\alpha_s g_{0s}\right] \quad \text{Eq. (12)}$$

Where,

$$\eta = \frac{(1+\alpha_s)}{2} \quad \text{Eq. (13)}$$

2.3.2 Granular Bulk Viscosity Model:

Lun et al. (1993) model for granular bulk viscosity is used in this numerical schemes and granular bulk viscosity is the function of dilatation.

$$\lambda_s = \frac{4}{3}\alpha_s \rho_s d_s g_{os}(1+e_s)\left(\frac{\Theta_s}{\pi}\right)^{\frac{1}{2}} \quad \text{Eq. (14)}$$

Where,

α_s in the Eq. (14) represents volume Fraction of the solid phase

e_s in the Eq. (14) represents the coefficient of restitution and in this modelling, we are using 0.95

d_s is the particle diameter, for the modelling of CFB, the diameter of solid particle used is 67μm

2.3.3 Radial Distribution:

The Syamlal o brien model is used which is a correction factor:

$$g_0(\alpha_s) = \frac{1}{1-\alpha_s} + \frac{\alpha_s}{2(1-\alpha_s)^2} \quad \text{Eq. (15)}$$

2.3.4 Solid Pressure:

Syamlal o brien model represented in Eq. (16) is the solid pressure for the CFB,

$$P_s = \alpha_s \rho_s \Theta_s(\omega + 2(1+e_s)\alpha_s g_{0s}) \quad \text{Eq. (16)}$$

$The\ value\ of\ \omega\ is\ 1\ for$ Syamlal o brien.

2.3.5 Elastic Modulus:

The Elastic modulus used in numerical scheme is derived type and represented its differential form in the Eq. (17) for $G \geq 0$

$$G = \frac{\partial P_s}{\partial \alpha_s} \quad \text{Eq. (17)}$$

2.4 Drag Model:

The drag model is used to capture the physics of interphase momentum transfer. The drag force is the force exerted by fluid on solid particle and when the drag force balance the weight of the particle the voidage increases. So, to capture this phenomenon the Syamlal drag model is used for modelling the circulating fluidized bed. The mathematical model given by Syamlal is given below.

$$K_{sg} = \frac{3\alpha_g \alpha_s \rho_g}{4 d_s {v^2}_r} C_D \left|\overrightarrow{u_s} - \overrightarrow{u_g}\right| \quad \text{Eq. (18)}$$

Where,

α_g is the volume fraction of gas

α_s is the volume fraction of solid

d_s is the diameter of the particle

$\left|\overrightarrow{u_s} - \overrightarrow{u_g}\right|$ is the absolute relative velocity

The drag factor is given by Dalla Valle

$$C_D = \left[0.63 + \frac{4.8}{\sqrt{\frac{R_e}{v_r}}} \right]^2 \quad \text{Eq. (19)}$$

The relative velocity v_r is modeled based on experimental data which is the work done by Richardson and Zaki. Garside and Al-Bibouni gave this model as below;

$$v_r = \frac{1}{2}[A - 0.06R_e] + \frac{1}{2}\sqrt{(0.06R_e)^2 + 0.12R_e(2B - A) + A^2} \quad \text{Eq. (20)}$$

Where,

$$A = {\alpha_g}^{4.14}$$

$$B = \begin{cases} 0.8{\alpha_g}^{1.28} & \alpha_g \leq 0.85 \\ {\alpha_g}^{2.65} & \alpha_g > 0.85 \end{cases}$$

The Reynolds number is given by the following relation:

$$R_e = \frac{\rho_g d_s \left|\overrightarrow{u_s} - \overrightarrow{u_g}\right|}{\mu_g} \quad \text{Eq. (21)}$$

2.5 Turbulent Model:

Different turbulent models are used for closure of this Reynold stress components. In this numerical simulation two equation model is used. The most used turbulent model in engineering application is two equation standard $k-\varepsilon$ model. This model solves the two-transport equation for each phase that is turbulent kinetic Energy and dissipation of energy. The general standard $k-\varepsilon$ model is given below:

The transport equation for turbulent kinetic energy for each phase is represented below:

$$\frac{\partial}{\partial t}\left(\alpha_q \rho_q k_q\right) + \nabla.\left(\alpha_q \rho_q \vec{U}_q k_q\right) = \nabla.\left(\alpha_q \frac{\mu_{t,q}}{\sigma_k} \nabla k_q\right) + \left(\alpha_q G_{k,q} - \alpha_q \rho_q \varepsilon_q\right) + \sum_{l=1}^{N} K_{lq}\left(C_{lq} k_l - C_{ql} k_q\right) - \sum_{l=1}^{N} K_{lq}(\vec{U}_l - \vec{U}_q).\frac{\mu_{t,l}}{\sigma_l \sigma_l} \nabla \alpha_l + \sum_{l=1}^{N} K_{lq}(\vec{U}_l - \vec{U}_q).\frac{\mu_{t,q}}{\sigma_q \sigma_q} \nabla \alpha_q \quad \text{Eq. (22)}$$

The transport equation for Dissipation of Energy is given represented below:

$$\frac{\partial}{\partial t}\left(\alpha_q \rho_q \varepsilon_q\right) + \nabla.\left(\alpha_q \rho_q \vec{U}_q \varepsilon_q\right) = \nabla.\left(\alpha_q \frac{\mu_{t,q}}{\sigma_\varepsilon} \nabla \varepsilon_q\right) + \frac{\varepsilon_q}{k_q}\left[\left(C_{1\varepsilon} \alpha_q G_{k,q} - C_{2\varepsilon} \alpha_q \rho_q \varepsilon_q\right) + C_{3\varepsilon}\left(\sum_{l=1}^{N} K_{lq}\left(C_{lq} k_l - C_{ql} k_q\right) - \sum_{l=1}^{N} K_{lq}(\vec{U}_l - \vec{U}_q).\frac{\mu_{t,l}}{\sigma_l \sigma_l} \nabla \alpha_l + \sum_{l=1}^{N} K_{lq}(\vec{U}_l - \vec{U}_q).\frac{\mu_{t,q}}{\sigma_q \sigma_q} \nabla \alpha_q\right)\right] \quad \text{Eq. (23)}$$

Where,

C_{lq}, C_{ql} *can be evaluated by the below formulae*:

$$C_{lq} = 2, C_{ql} = 2\left(\frac{\eta_{lq}}{1+\eta_{lq}}\right) \quad \text{Eq. (24)}$$

Where,

η_{lq} *is the ratio of two integral time scales which is given below*

$$\eta_{lq} = \frac{\tau_{t,lq}}{\tau_{F,lq}}$$

μ_t *is the turbulent kinetic energy also called reynold stress components*

$C_{1\varepsilon}, C_{2\varepsilon}, C_{3\varepsilon}$ *are constants*

$G_{k,q}$ *is the generation of turbulent kinetic energy*

2.6 Near Wall Treatment:

This project involves the effect of near wall treatment on hydrodynamic properties of the circulating fluidized. The different wall function models are tested to study these effects near the wall. The flow near the wall is very different from the core annulus flow because near the wall the viscous stresses are more dominant as compared to fluctuating or turbulent components because of no slip and no penetration boundary conditions. Our main aim of the study is to test different wall function model and compare the numerical results with the experimental results to check the behavior of solid holdup and particle velocity very close to the wall. The near wall treatment depends on the Y^+ value. Y^+ value is the dimensionless height from the wall where the viscous stresses are dominant. Depending on this value different layers can be described as shown in the figure:

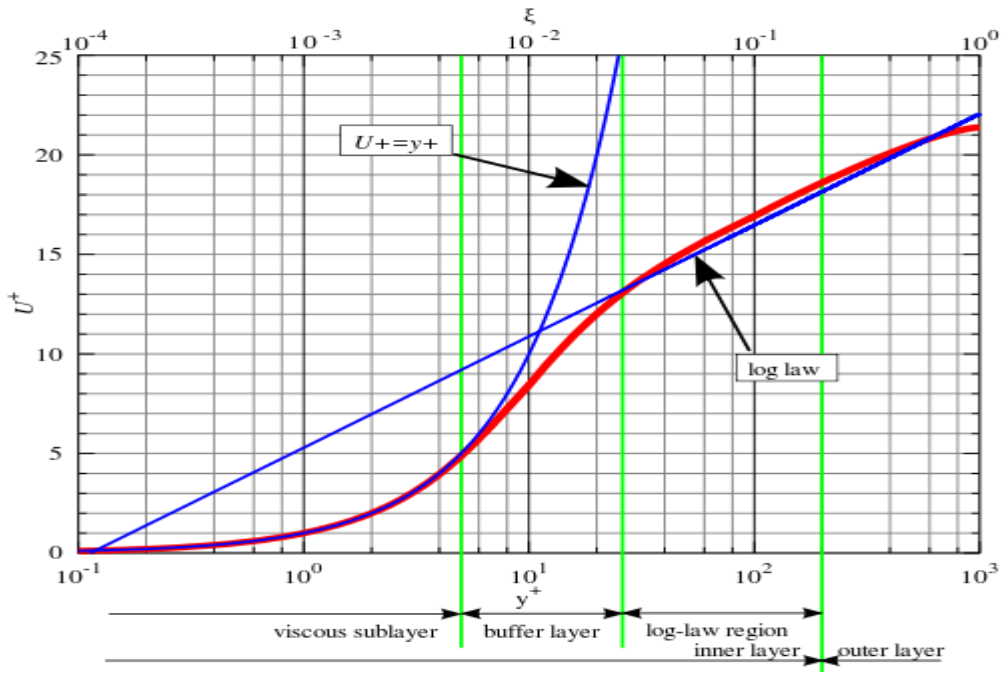

[2]Fig. (3)

The Fig. (1) shows the plot between Y^+ and U^+. The plot is divided into three layers that are viscous effects, buffer layer and outer layer. There is overlap region where can apply log law. In fluent near wall treatment based on models that are represented based on two-layer zone and log law and Reynolds number. Because near the wall Reynolds number is low some models used blending function to transition from higher Reynolds number to lower Reynolds number. However, the two-layer zone is more popular for near wall treatment because if Reynold number

[2] The above figure is taken from https://upload.wikimedia.org/wikipedia/commons/thumb/4/4c/Law_of_the_wall_%28English%29.svg/500px-Law_of_the_wall_%28English%29.svg.png

is low as 100 the blending function treated as near wall but it is far away from the wall. The viscous sublayer is dominant when $Y^+ < 5$, when, $5 \leq Y^+ \leq 30$ is known as the buffer layer. In buffer layer, the profile is neither linear nor logarithmic and when, $Y^+ > 30$ This is known as logarithmic zone.

In this numerical simulation of circulating fluidized bed, the mesh is created based on the $Y^+ \sim 1$ to capture all the physics near the wall. Three wall function models are used as given below:

a) Standard wall functions
b) Scaleable Wall Functions
c) Menter Lechner Wall Functions

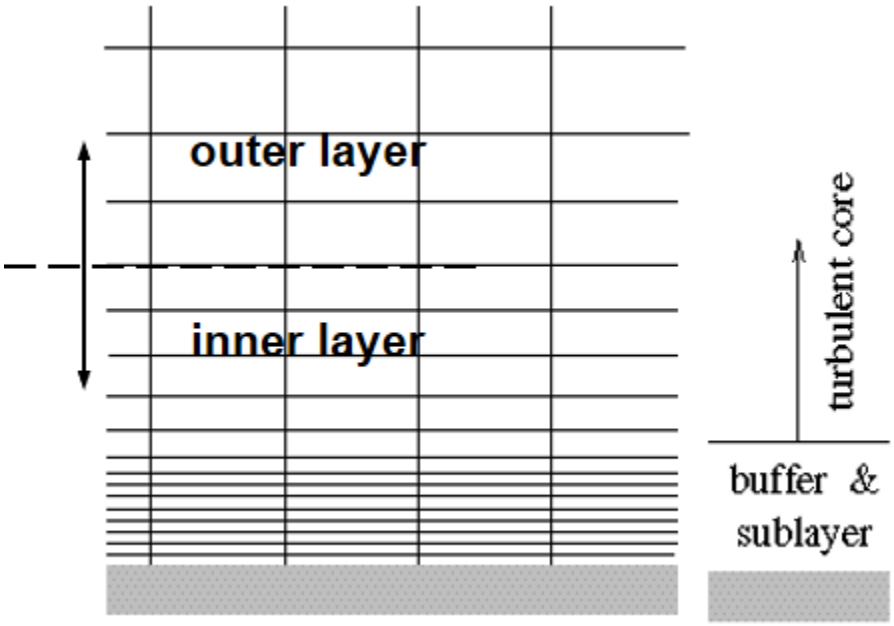

[3]Fig. (4) Mesh Layering

2.6.1 Standard wall functions:

In standard wall functions, the near wall treatment captures from two explicit correlations depending upon the Y^+ value which is given below:

$$Y^+ = \frac{\rho {C_\mu}^{1/4} {k_p}^{1/2} y_p}{\mu} \rightarrow \begin{cases} Y^+ \geq 11.225, \; U^+ = \frac{1}{k}\ln(EY^+) \\ Y^+ < 11.225, \; U^+ = Y^+ \end{cases} \rightarrow \tau_w = \frac{U_p {C_\mu}^{1/4} {k_p}^{1/2}}{\frac{U^+}{\rho}} \qquad \text{Eq. (25)}$$

Where,

U_p is the velocity in the center of the cell near the wall
y_p is the vertical distance from the cell center from the wall
k_p is the turbulent kinetic energy

[3] http://www.petrodanesh.ir/Virtual%20Education/Mechanics/ANSYS-FLUENT/ANSYS%20CO/fluent12-lecture06-turbulence.ppsx

k is the von kamran constant and its value is 0.41
E is empirical constant and its value is calculated based on surface condition

For smooth surface its value is 9.8.

From the Eq. (25) there are two correlations are used in standard wall functions that is when $Y^+ \geq 11.225$ the log law will be used for near wall treatment and $Y^+ < 11.225$ a linear profile is used to treat the near wall effect. The standard wall function is mostly used in engineering applications for its higher computational speed.

2.6.2 Scalable Wall Functions:

The scalable wall functions are the modified form of the standard wall functions. In the standard wall functions when the $Y^+ < 11.225$ then standard wall function not gives good results for near wall treatment. Therefore, when the $Y^+ < 11.225$ the scalable wall functions uses the log law to treat the near wall effects. The scalable wall functions are used along with standard wall function by using the below limit value which is given by:

$$Y^+ = MAX(Y^+, {Y^+}_{limit}) \quad \text{Eq. (26)}$$

Where,

$${Y^+}_{limit} = 11.225 \quad \text{Eq. (27)}$$

2.6.3 Menter Lechner Wall Functions:

In the enhanced wall treatment, the treatment of the near wall effects is based on the two layer zones. The one layer which is viscosity effected zone and second layer is where the flow is fully turbulent. The switching between these layers depends upon the turbulent Reynolds number. The major drawback of switching based on turbulent Reynolds number is that it can switch even when the Reynolds number is 100 and it may be far away from the wall in actual. Therefore, a new model has been developed that is not based on 2-layer zone. The Menter-Lechner wall functions adds a source term in the transport equation that will consider the near wall treatment as shown below:

The transport equation for turbulent kinetic energy in addition with near wall source term which can be written as based on Menter Lechner Model:

$$\frac{\partial}{\partial t}(\rho k) + \frac{\partial}{\partial x_i}(\rho k u_i) - \frac{\partial}{\partial x_j}\left[\left(\mu + \frac{\mu_t}{\sigma_k}\right)\frac{\partial k}{\partial x_j}\right] = G_k - \rho\varepsilon + S_{near-wall} \quad \text{Eq. (28)}$$

The transport equation for dissipation of turbulent kinetic energy which can be written as

$$\frac{\partial}{\partial t}(\rho\varepsilon) + \frac{\partial}{\partial x_i}(\rho\varepsilon u_i) - \frac{\partial}{\partial x_j}\left[\left(\mu + \frac{\mu_t}{\sigma_\varepsilon}\right)\frac{\partial k}{\partial x_j}\right] = C_{1\varepsilon}\frac{\varepsilon}{k}G_k - C_{2\varepsilon}\rho\frac{\varepsilon^2}{k} \qquad \text{Eq. (29)}$$

Where,

$S_{near-wall}$ *is the source term which is used to treat the near wall effects*

$\mu_t = \rho C_\mu \frac{k^2}{\varepsilon}$ is the turbulent stress

$C_{1\varepsilon}, C_{2\varepsilon}, C_\mu, \sigma_k, \sigma_\varepsilon$ *are consatnts and values are* 1.44,1.92,0.09, 1.0 *and* 1.3 *respectively*

Chapter 3: Numerical Schemes

This project involves the modelling and 2-D simulation of the riser part of the circulating fluidized bed to study the effect on hydrodynamic properties near the wall zone using three different wall functions. The simulations were performed on riser which is 10 m long and 0.0762 m wide. The riser is symmetric about an axis and domain was considered is from -0.0381 to 0.0381. The detailed geometry and boundary conditions for a riser are shown in the below Fig. (5)

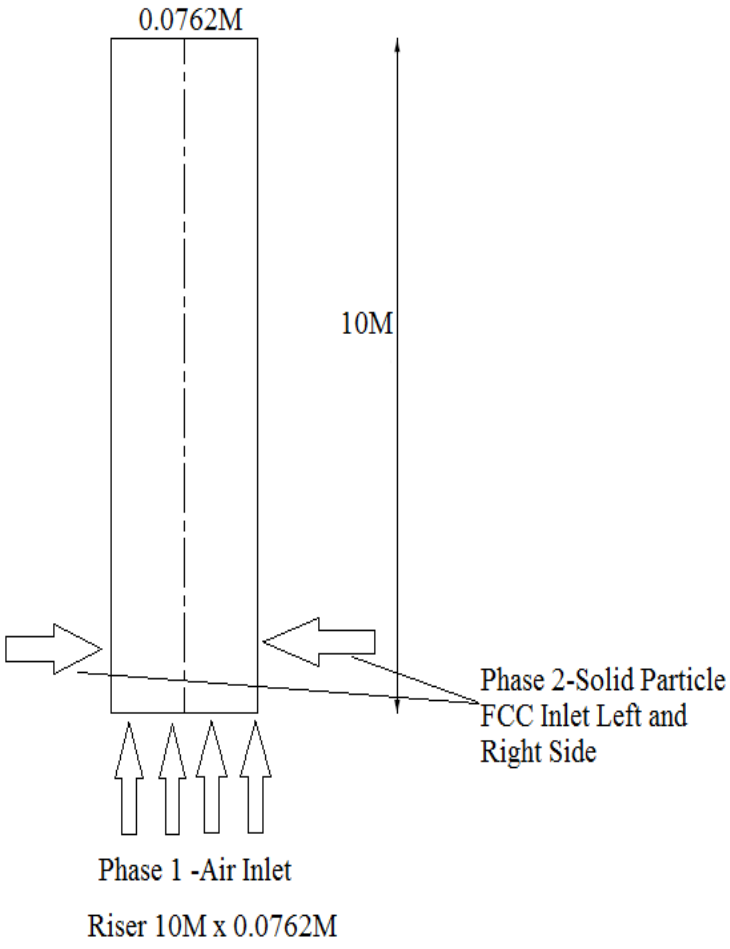

Fig. (5) Geometry and Boundary Conditions

The simulations were performed using Eulerian-Eulerian method along with granular model for solid phase. The superficial gas velocity 5 m/s was used for phase 1 as velocity inlet condition and gas is supplied from the bottom of the riser and therefore volume fraction is 0 for the solid phase at the bottom of the riser. The solid is circulated from right and below side of the wall as shown in the Fig. (3). The no slip boundary condition is used for gas phase on the right and left wall but for solid phase the specularity coefficient is defined and specularity coefficient of 0.0001 was used in

this simulation and for Collison model a restitution coefficient was defined as 0.95. The initial packing of the solid phase is 0.63 is defined in the software. The outflow type outlet boundary conditions were used. The same geometry and mesh are created in the ICEM as shown in the Fig. (3). The mesh is created based on the Y^+=1 and corresponding first spacing near the wall is given below:

$$\Delta s = 0.000078$$

The grid consists of 564960 nodes based on Y^+=1 as shown in Fig. (6)

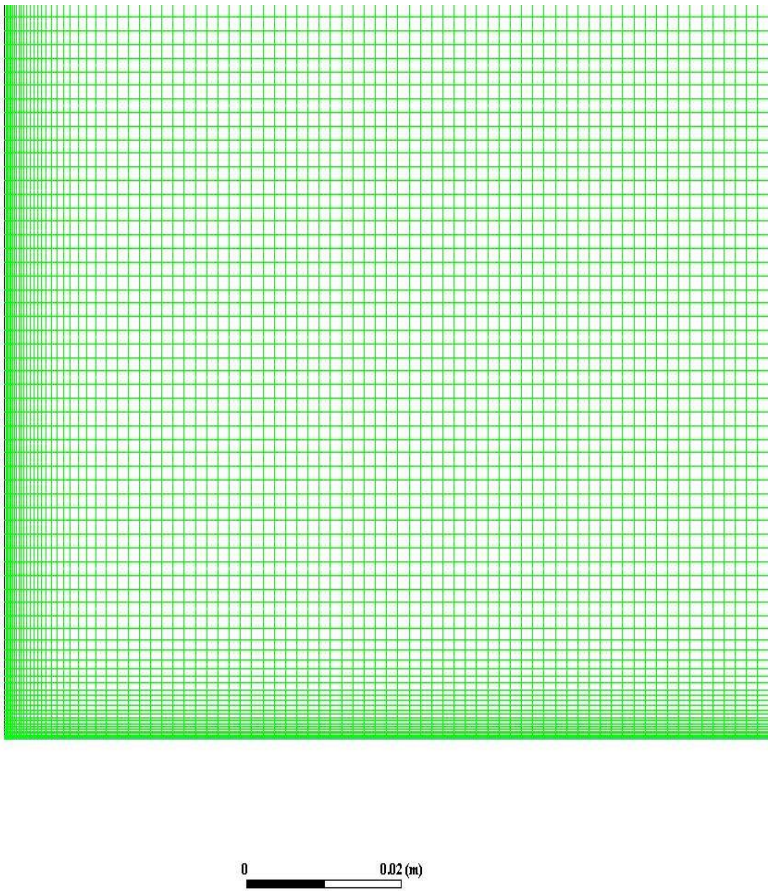

Fig. (6) Grid Size and Refined near the wall based on $\Delta s = 0.000078$

The numerical solutions were obtained based on Eulerian-Eulerian model with granular model for solid phase. The turbulence of the flow in the core annulus is captured using the most used in the industrial application is standard $k - \varepsilon$ model. The transport equation for turbulent kinetic energy and dissipation of energy is solved for each phase as shown in the Eq. (22) and Eq. (23). The focus of this project to capture near wall effects on hydrodynamics of CFB therefore three different models namely standard, scalable, Menter-Lechner wall functions were tested along with standard $k - \varepsilon$ model. The pressure-velocity coupling is solved by phase coupled simple algorithm that is a modified version of SIMPLE algorithm for two phase flow. In coupled phase condition, the solver will compute pressure-velocity coupling using implicit method. The spatial discretization

was done using different schemes for different governing equation as shown in Table. (2). The Power law discretization schemes are used because of it higher accuracy than the second order upwind scheme except for volume fraction governing equation the QUICK scheme is used for discretization. All the parameter for gas and solid phase that was used in these simulations are detailed in the Table (3). The transient simulation was done on fixed time step of 1e-05.

Table 2. Numerical Schemes for Governing Equations

Spatial Discretization	**Numerical Schemes**
Gradient	Green Gauss Cell based
Momentum	Power Law
Volume fraction	Quick
Granular Temperature	Power Law
Turbulent Kinetic Energy	Power Law
Turbulent Dissipation Rate	Power law

Table 3. Boundary Conditions and Simulation Parameters

Particle Properties	**Values**
1. Particle(FCC) Density	1500 kg/m^3
2. Gas (Air) Density	1.225 kg/m^3
3. Particle Diameter	67μm
4. Superficial Gas Velocity	5 m/s
5. Specularity Coefficient	0.0001
6. Coefficient of Restitution	0.95
7. Wall boundary condition	No-Slip for Gas Phase
8. Wall boundary condition	Slip Boundary
9. Inlet Boundary condition	Velocity Inlet (Gas and Solid)
10. Outlet Boundary condition	Outflow
11. Mesh Domain	10 x 0.0762 Meter
12. Width domain	-0.0382 to 0.0381 Meter
13. Packing Limit	0.63
14. Solid Circulation Rate G_s	100 kg/m^{2}s

Chapter 4: Results and Discussions

4.1 Grid Independence Test:

The grid independence test was done on three different grids and the work for the same has already been completed by "Zeneng Sun" a PhD candidate in the University of Western Ontario. The size and quality of a grid that was chosen for simulation is shown in Table. (4) and Table. (5) respectively.

Table. 4 Grid Size

Levels	0
Cells	560133
Faces	1125092
Nodes	564960
Partitions	1

Table. 5 Mesh Quality

Quality Criterion	Values
Minimum Orthogonal Quality	1.00000e+00
Maximum Ortho Skew	0.00000e+00
Maximum Aspect Ratio	2.74373e+01

4.2 Results and Discussion:

The Post processing has been done in the Fluent 16.2. All the results are time-averaged at 0.5,1.0,1.5,2.0, 2.5 and 3.0 seconds. The plots of solid hold up and particle velocity has been plotted along the radial distance of the riser at different heights and compared with experimental data. The main focus of the study is to check the near wall effects on solid hold up and particle velocity near the wall using three different wall function. From Fig. (7) it can be clearly seen that at 1.96-meter height of the riser the solid hold up near the wall is more as compared to the other location along the radial direction as depicted by all the three models and experimental studies. The standard and scalable wall function shows the similar trend and the magnitude of solid hold is almost same in both the models but Menter Lechner model depicted more close magnitude when compared with the experimental results. At 2.42-meter height of the riser, the standard and scalable model shows some fluctuations this may be due to low flow time and flow did not reach pseudo-transient state. However, the Menter-Lechner model again remains the stable and accurate when compared with the experimental results. Similar trend can be seen in Fig. (9) and Fig. (10) at height of 4.81-meter and 7.35 meter of height. From Fig. (7) to Fig. (10) the results are plotted by marking

the rake along the radial direction from center to the near of the wall like 0.0 to 0.0361 meter at different heights of the riser.

From Fig. (11) to Fig. (14) the results are plotted to check the near wall effects and the rake was marked from r/R from 0.82 to 0.98 at different heights of the riser. In all the cases, the Menter Lechner model higher values of solid hold up near the wall. Therefore, we can say that Menter Lechner wall is the most accurate wall function as compared with standard and scalable wall functions.

From Fig. (15) to Fig. (18), the results are plotted to check the particle velocity at different heights of the riser along the radial direction. From the Fig. (15), It can be clearly seen that the particle velocity at the center of the riser is more as compared with near the wall at 1.96 meter of height. The particle velocity decreases near the wall. In experimental results, the velocity is negative at 2.88-meter height because cluster of particles is the near the wall and they just slide down very near the wall. In our models, we defined very low coefficient of restitution that is 0.0001 that depicts positive velocity vector near the wall. However, there are also negative velocity vector very close the solid inlet as shown in velocity vector Fig. (24). From Fig. (15) to Fig (18), Menter Lechner model proved to be the best fit between experimental and numerical results as compared with standard and scalable wall functions. For closer view near the wall, the rake is drawn near wall along the radial direction from r/R 0.82 to 0.98 and compared three different models, the Menter Lechner Model depicted higher values in most of the cases as shown in Fig. (19) to Fig. (22).

The Fig. (23), Fig. (25) and Fig. (26) shows contours of the volume fraction of solid particle for three different wall functions namely standard, scalable and Menter Lechner model. The contours are shown at different times at 0.5,1.0,1.5,2.0,2.5 and 3.0 seconds. The solid volume fraction near the wall is more as compared to center location of the riser as depicted by all the three models but the Menter-Lechner Model depicted the best fit with the experimental data.

4.3 Conclusions

The simulation was performed using three different near wall treatment functions, Standard, Scalable wall function respectively. These numerical results then compared with experimental data on the hydrodynamics of the circulating fluidized bed. On comparing different near wall treatment models with experimental data, the key conclusion is that the Menter Lechner model shows good agreement with experimental results on solid holdup and particle velocity near the wall zones at different heights of the circulating fluidized bed. The solid hold up is maximum near the wall zones and clusters of solid can be seen from the contours of volume fractions. On the other hand, the particle Velocity is maximum at the center of the riser and goes on decreasing along the radial direction to the wall. Some deviation has been seen in the figures for solid hold up and particle velocity with experimental studies. This might be due to that the simulation flow time did not reached the pseudo-transient state.

4.4 Future Work

We can compare the Enhanced wall treatment with the other three models and all these near wall treatments based on two-layer zone or low Reynolds number. We can try three-layer wall zone function by writing a UDF code and compare with other models. The Buffer-layer is neither linear nor logarithmic profile so we consider it is as polynomial function and implemented in the Fluent using UDF. The UDF code is written for three-layer zone is given below:

```
#include "udf.h"
DEFINE_WALL_FUNCTIONS(user_log_law, f, t, c0, t0, wf_ret, yPlus, Emod)
{
real wf_value;
switch (wf_ret)
 {
case UPLUS_LAM:
wf_value = yPlus;
break;
case UPLUS_TRB:
     if (5 < yPlus && yPlus < 30)
     {
               wf_value = -1.1297 + 1.4676*yPlus - 0.0515*yPlus*yPlus +
0.0006*yPlus*yPlus*yPlus;

     }
     else
     if (yPlus >= 30)
     {
       wf_value = log(Emod*yPlus)/KAPPA;
     }
break;
case DUPLUS_LAM:
wf_value = 1.0;
break;
case D2UPLUS_TRB:
wf_value = -1./(KAPPA*yPlus*yPlus);
 break;
default:
 printf("Wall function return value unavailable\n");
 }
 return wf_value;
}
```

5. Tables and Graphs:

5.1 Solid Hold Up from Center to the Near wall at different heights of the Riser

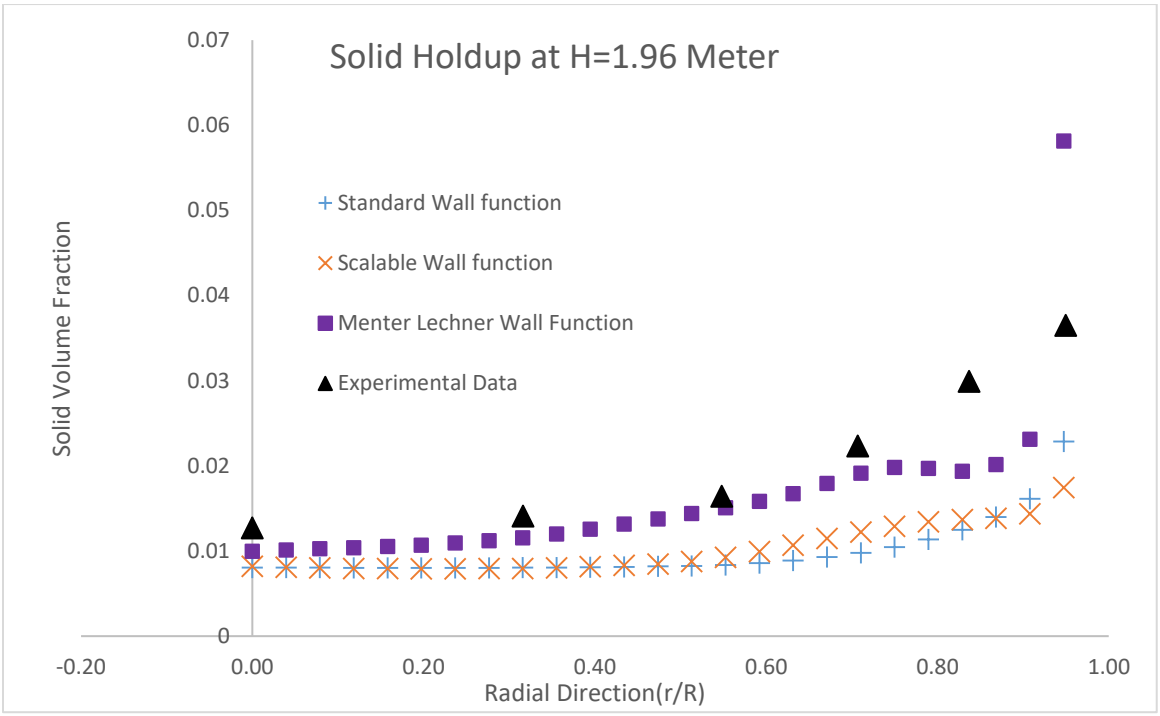

Fig. (7) Solid Hold Up along a Radial Direction from center to Near wall at H=1.96 M

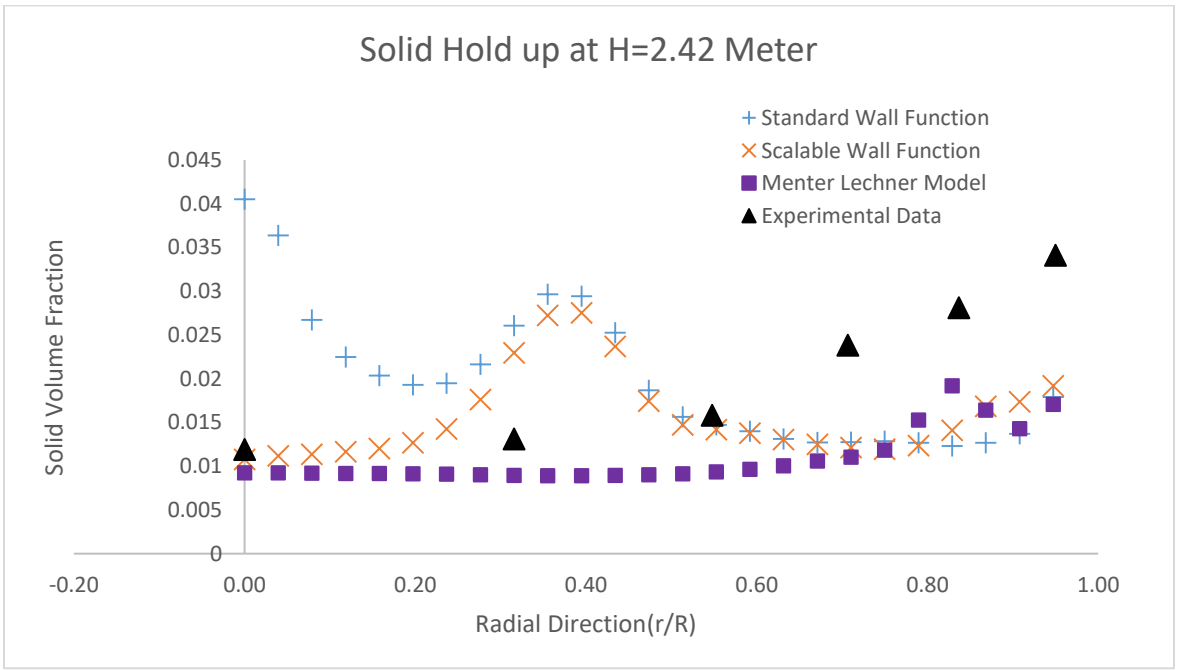

Fig. (8) Solid Hold Up along a Radial Direction from center to Near wall at H=2.42 M

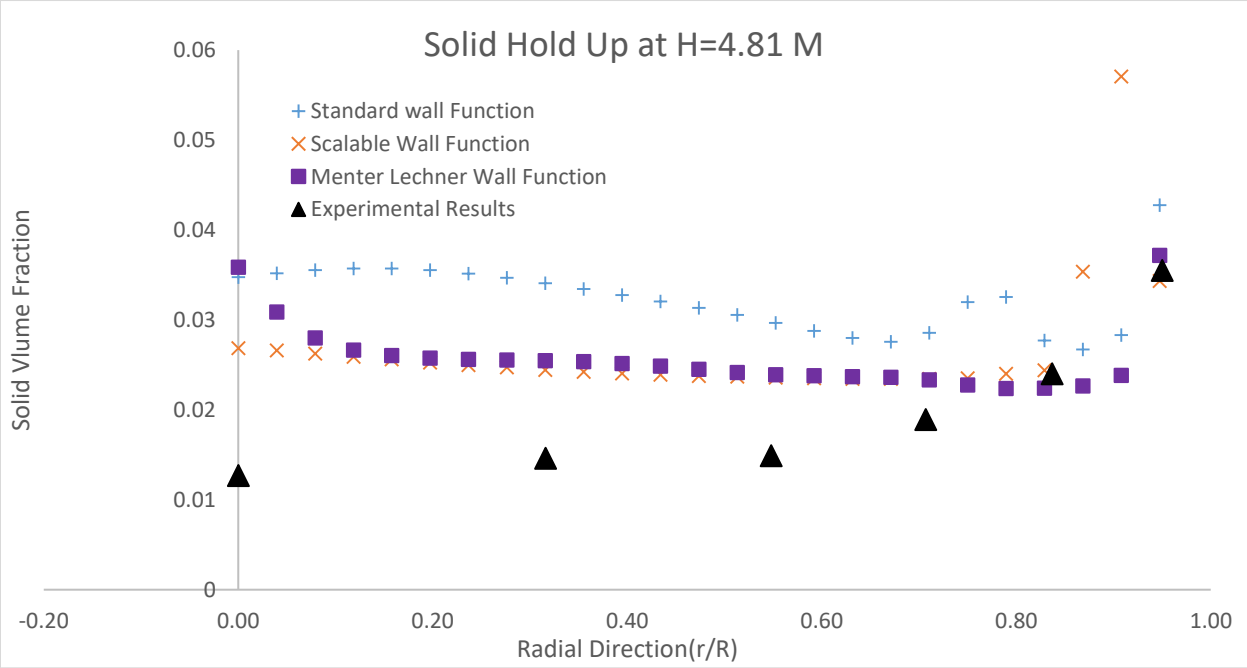

Fig. (9) Solid Hold Up along a Radial Direction from center to Near wall at H=4.81 M

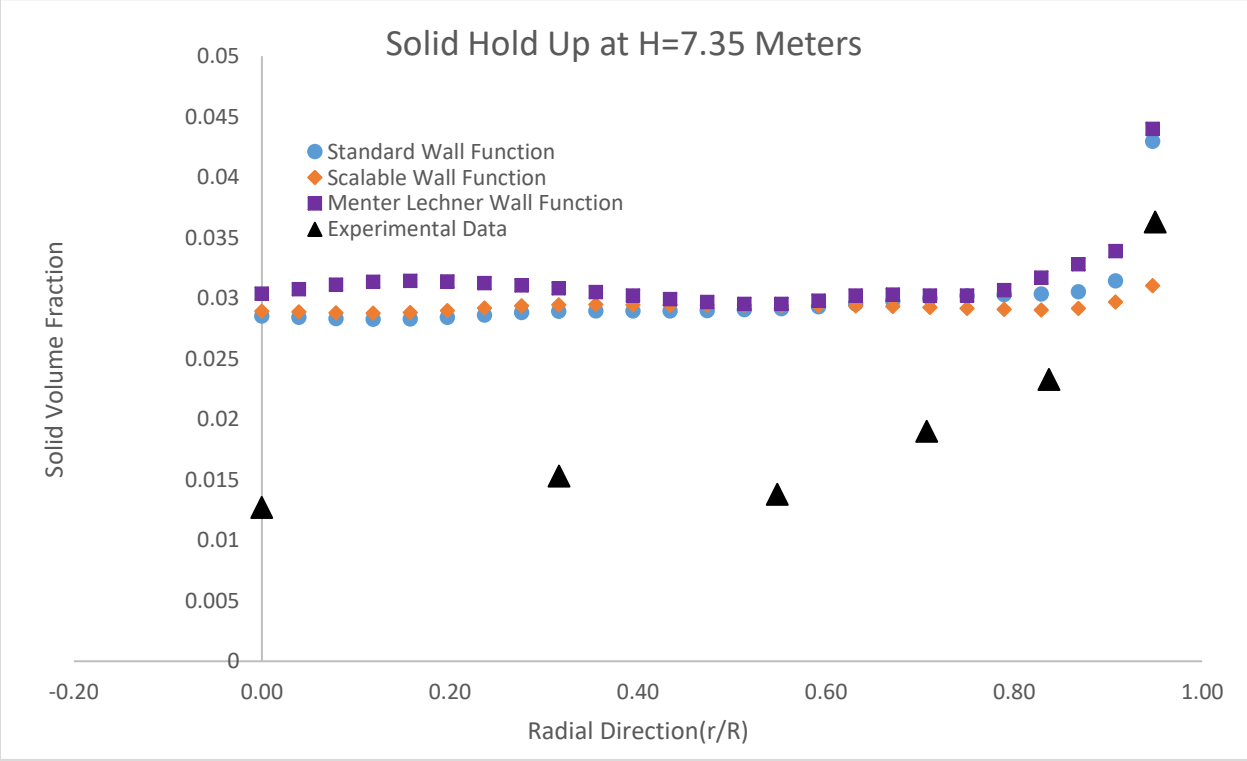

Fig. (10) Solid Hold Up along a Radial Direction from center to Near wall at H=7.35 M

5.2 Solid Hold Up very close to wall along the Radial Direction at different heights:

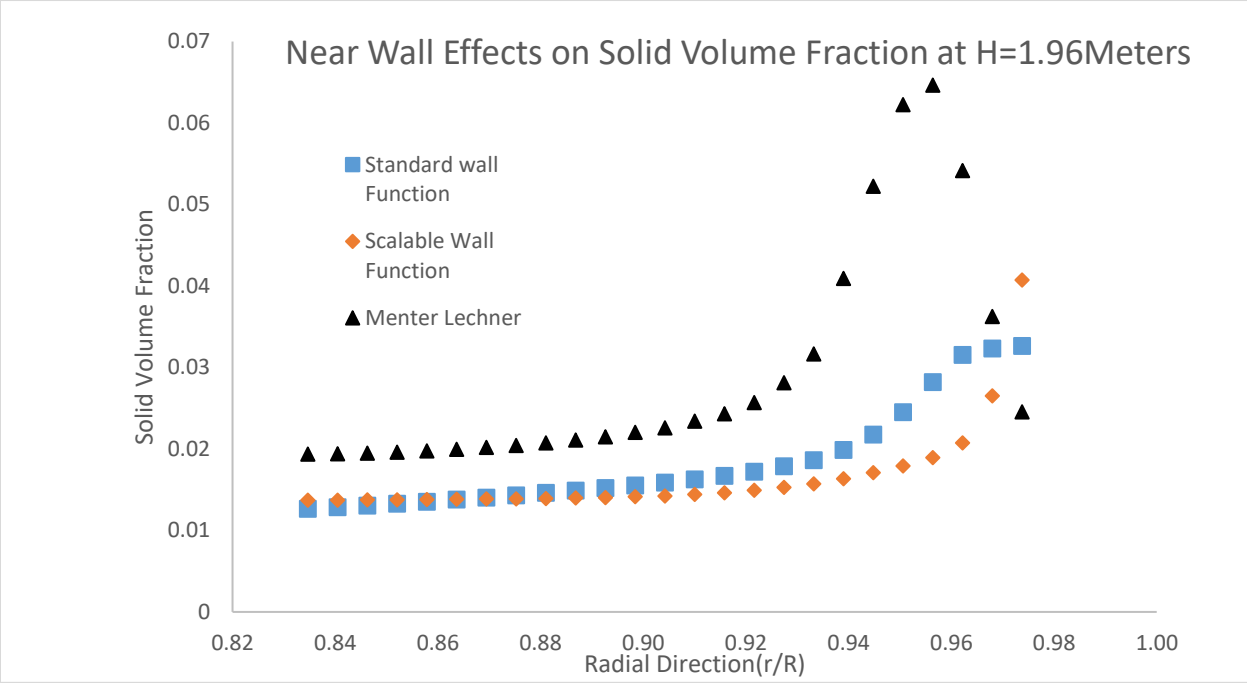

Fig. (11) Solid Hold Up along a Radial Direction very close to the Wall at H=1.96 M

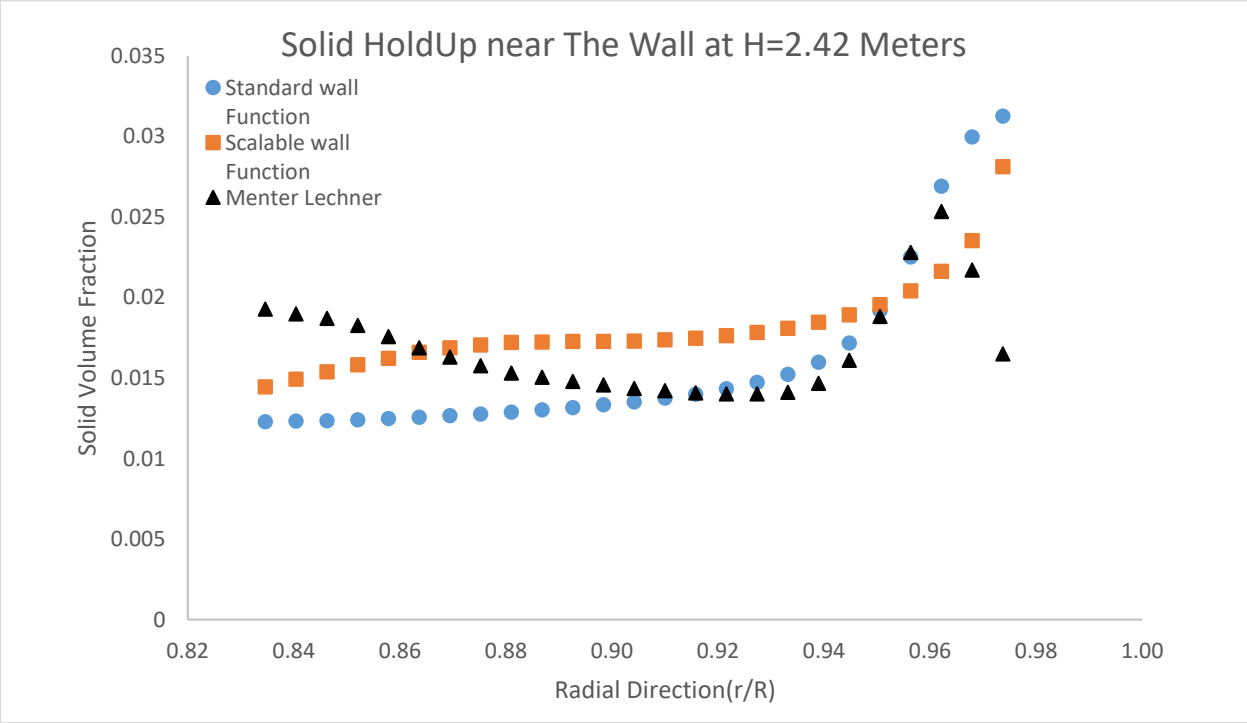

Fig. (12) Solid Hold Up along a Radial Direction very close to the Wall at H= 2.42 M

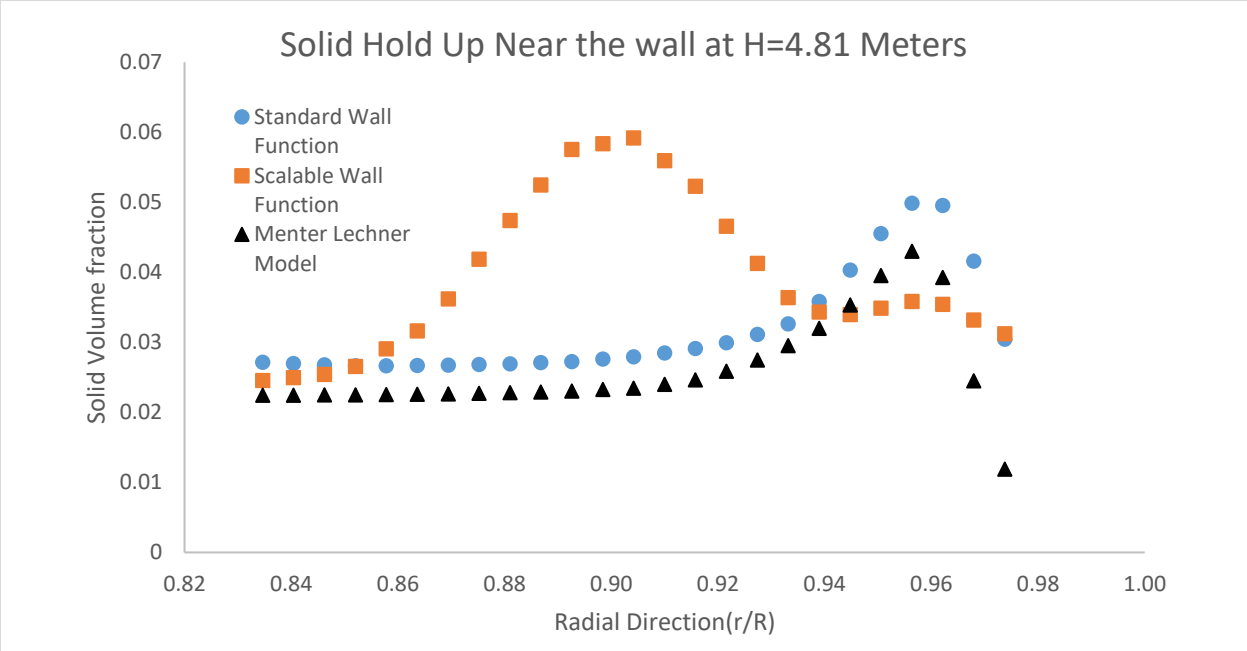

Fig. (13) Solid Hold Up along a Radial Direction very close to the Wall at H= 4.81 M

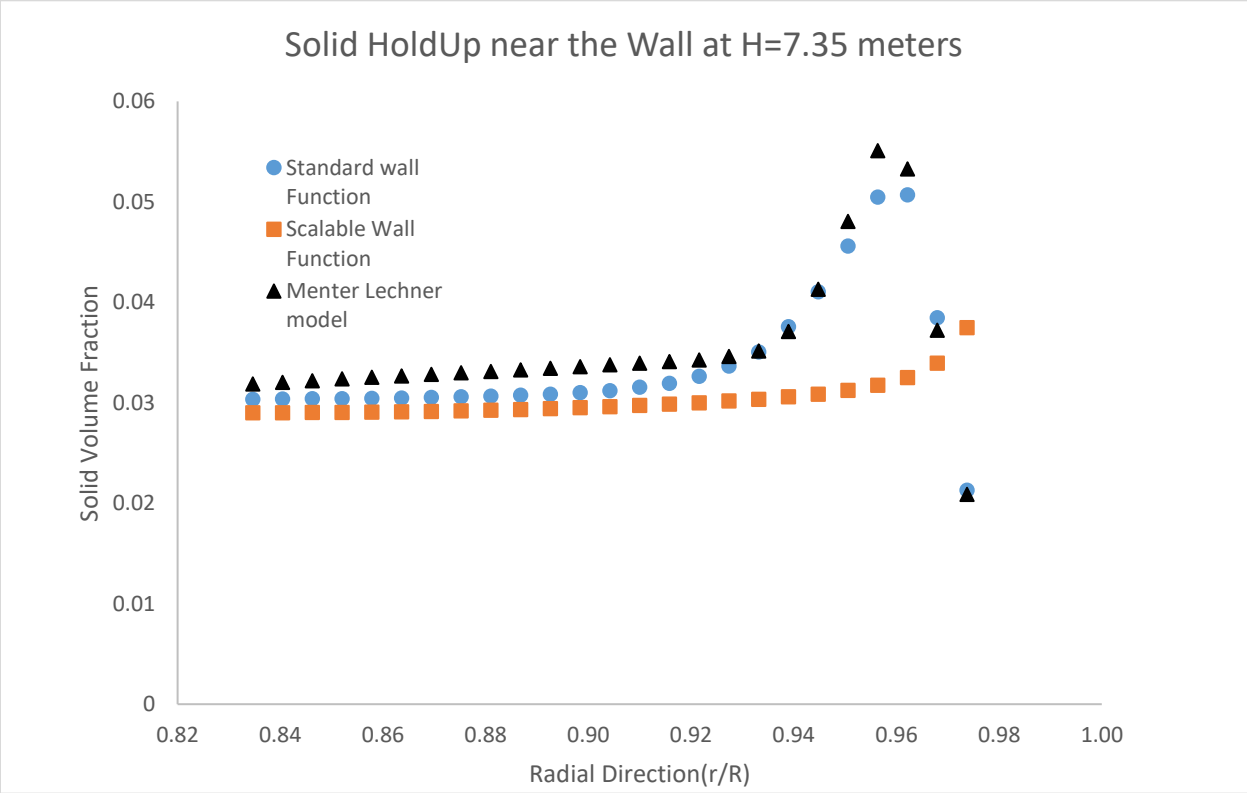

Fig. (14) Solid Hold Up along a Radial Direction very close to the Wall at H=7.35 M

5.3 Particle Velocity from center to near the wall along the Radial Direction at different heights:

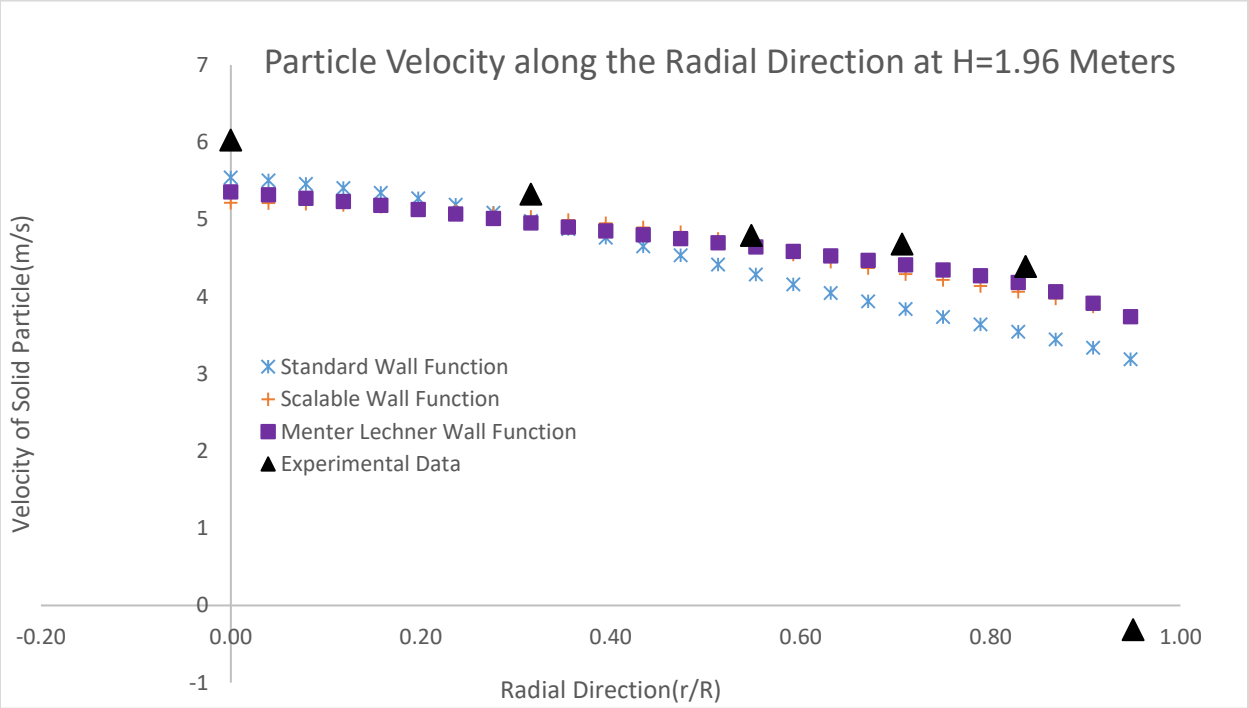

Fig. (15) Particle Velocity along the radial direction at H=1.96 M

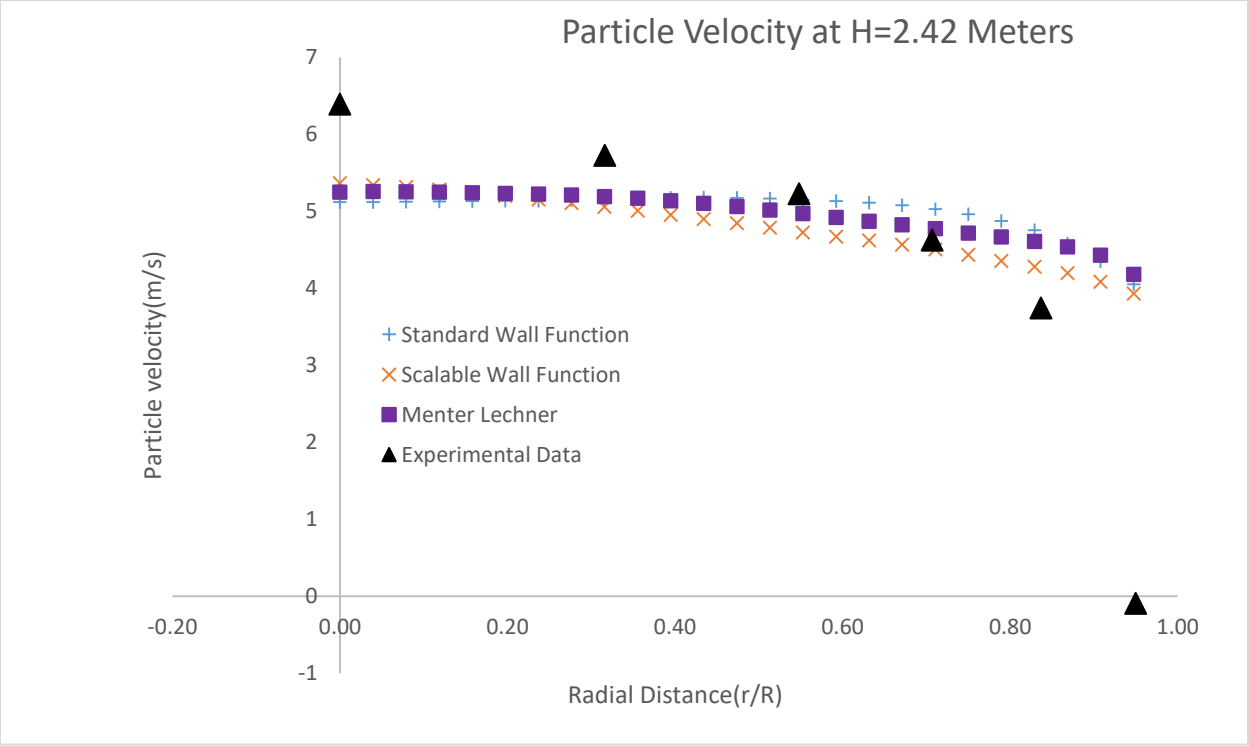

Fig. (16) Particle Velocity along the radial direction at H=2.42 M

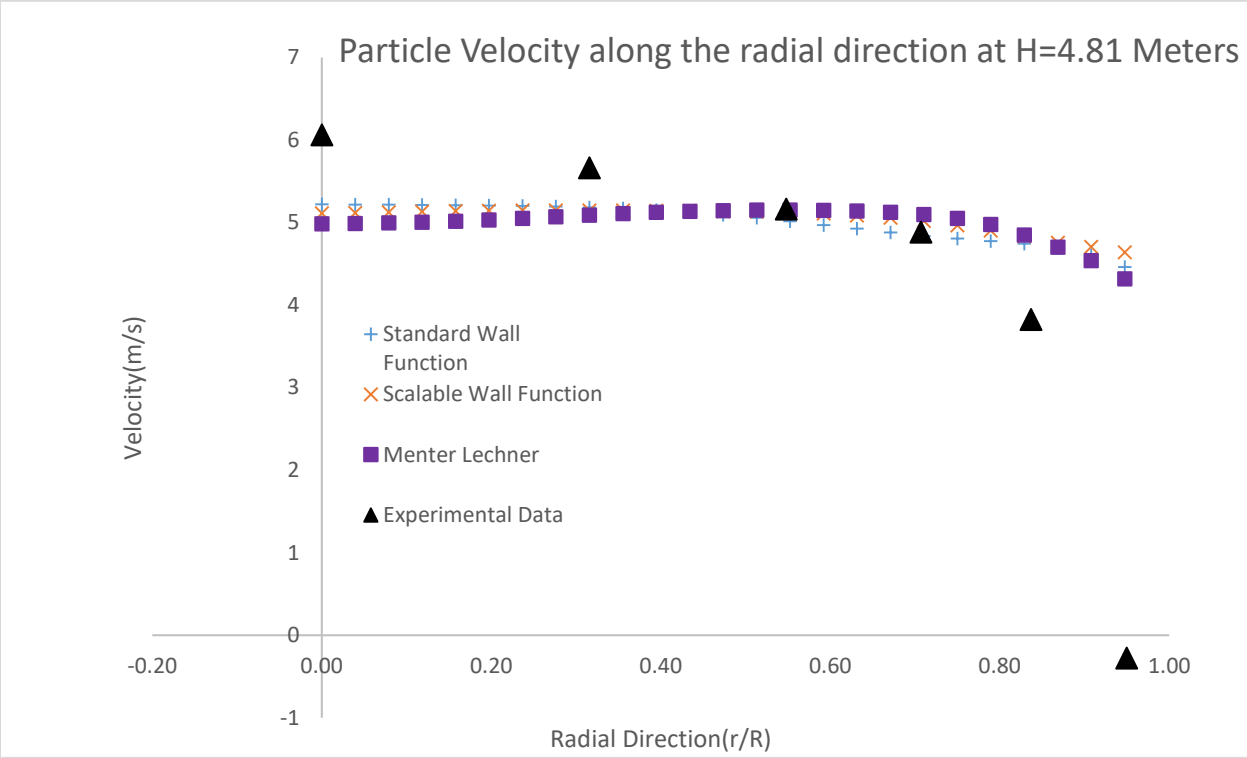

Fig. (17) Particle Velocity along the radial direction at H=4.81 M

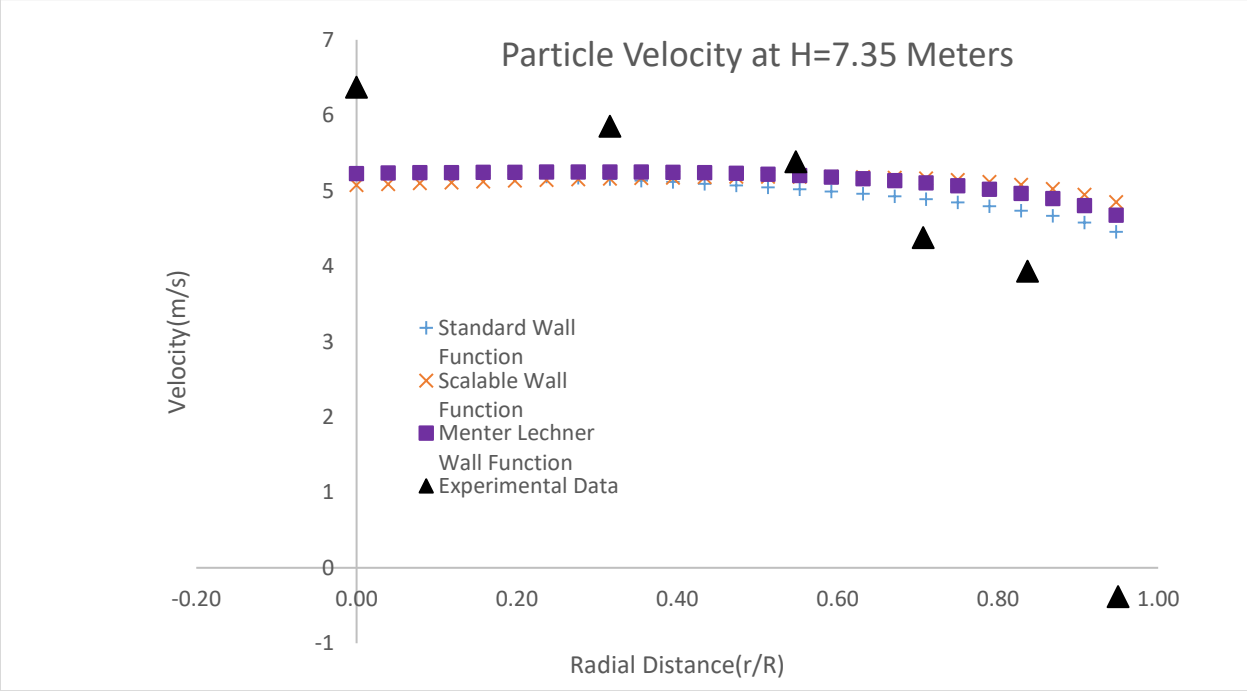

Fig. (18) Particle Velocity along the radial direction at H=7.35 M

5.4 Particle Velocity very close to the wall along the Radial Direction at different heights:

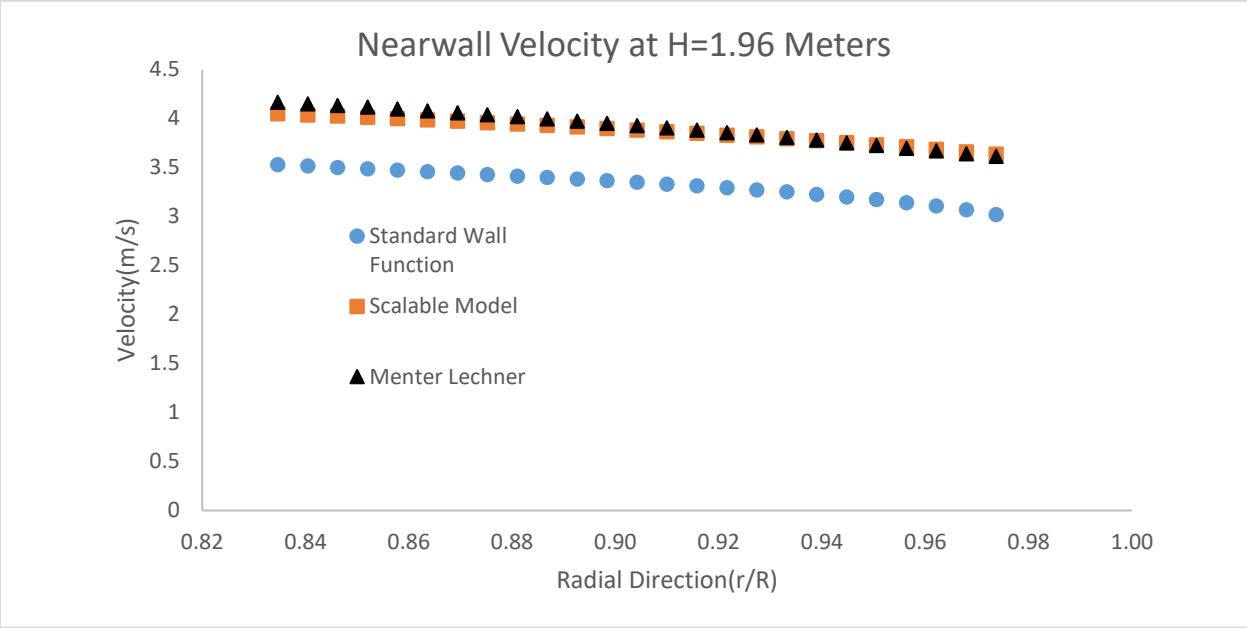

Fig. (19) Particle Velocity very close to the wall along the radial direction at H=1.96 M

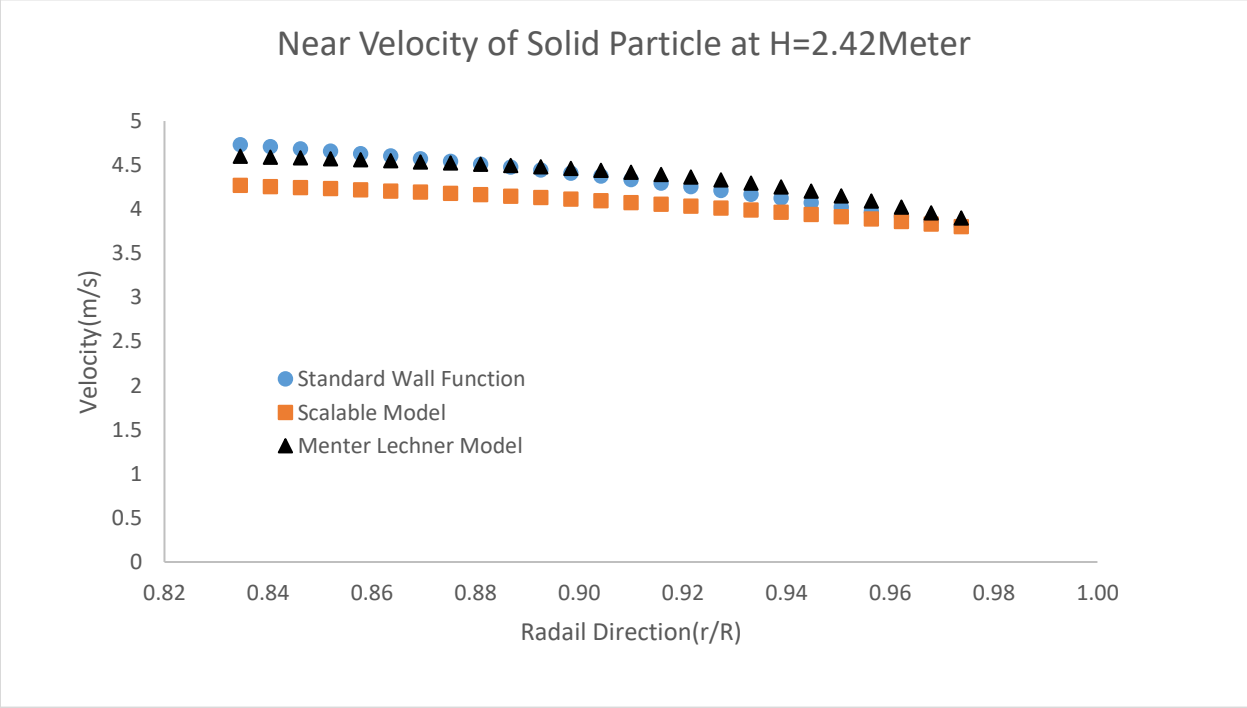

Fig. (20) Particle Velocity very close to the wall along the radial direction at H=2.42 M

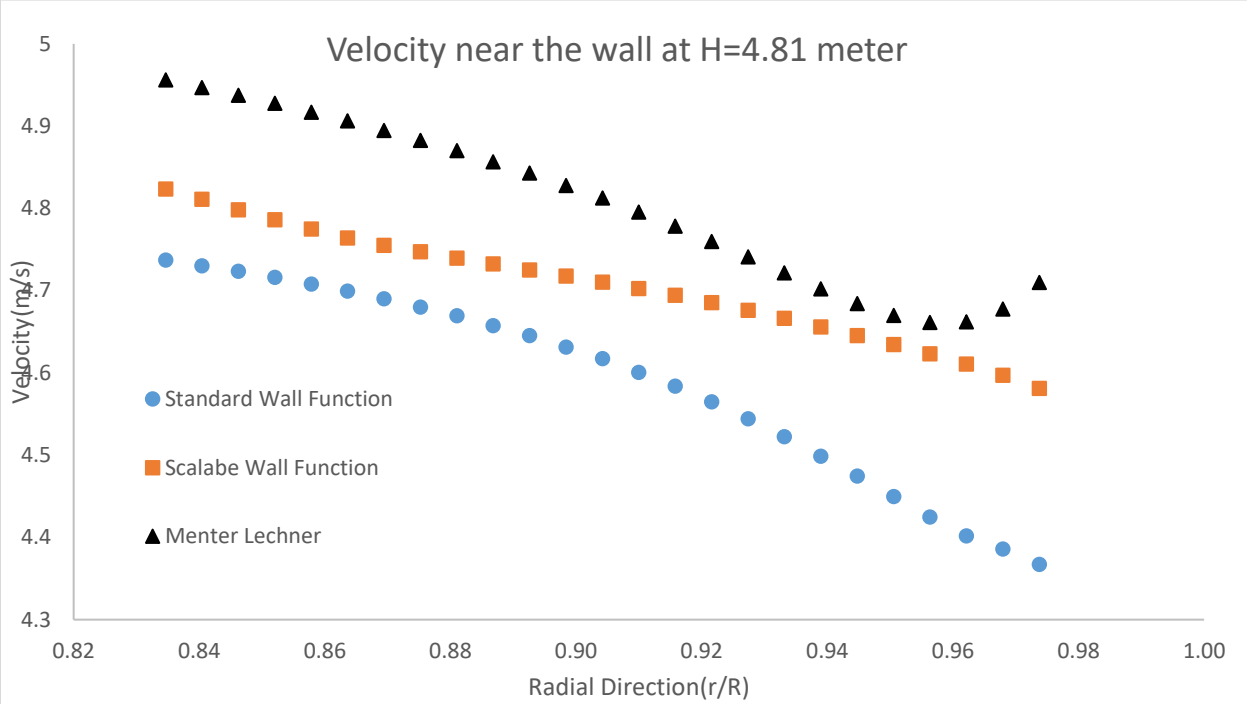

Fig. (21) Particle Velocity very close to the wall along the radial direction at H=4.81 M

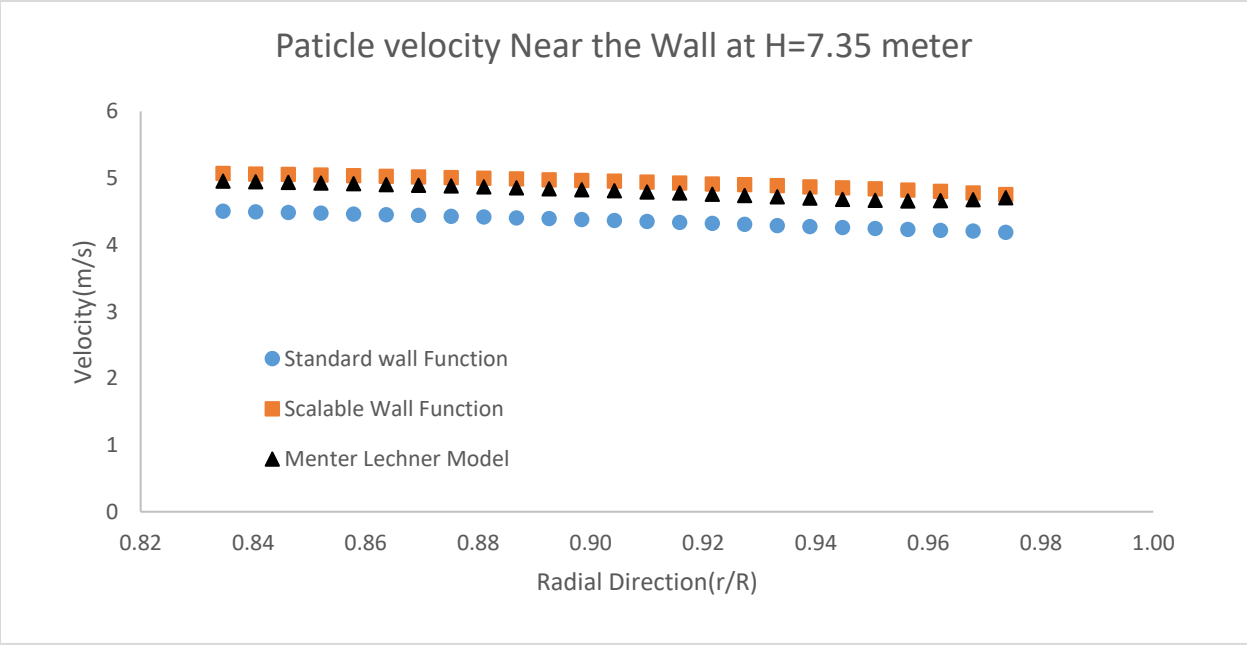

Fig. (22) Particle Velocity very close to the wall along the radial direction at H=7.35 M

5.5 Volume Fraction of the solid phase at different times and shows the flow development:

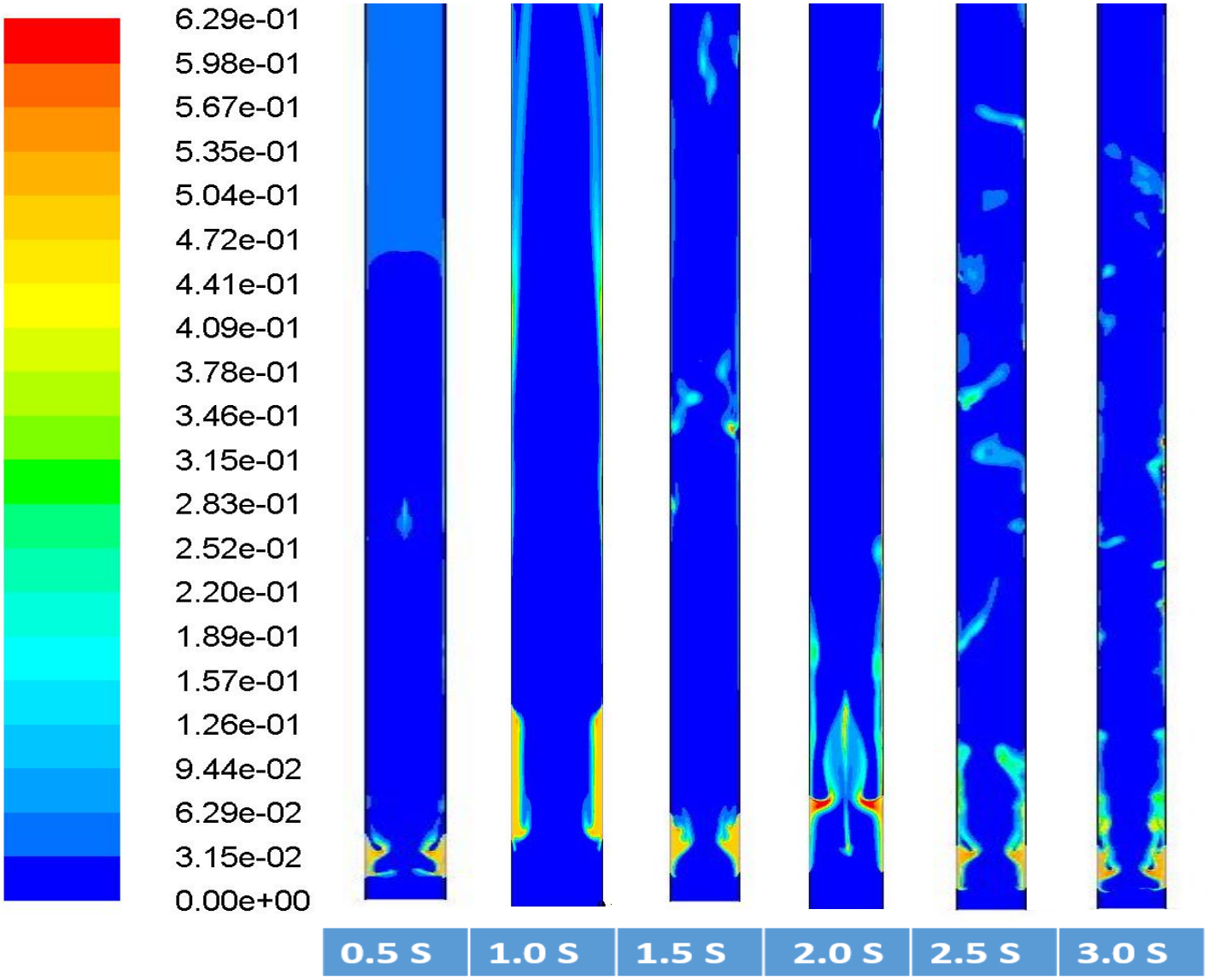

Fig. (23) Solid Particle Suspension using **Standard Wall Function** at Different times

5.6 Velocity Vector field and showing velocity direction very-very close to the Wall:

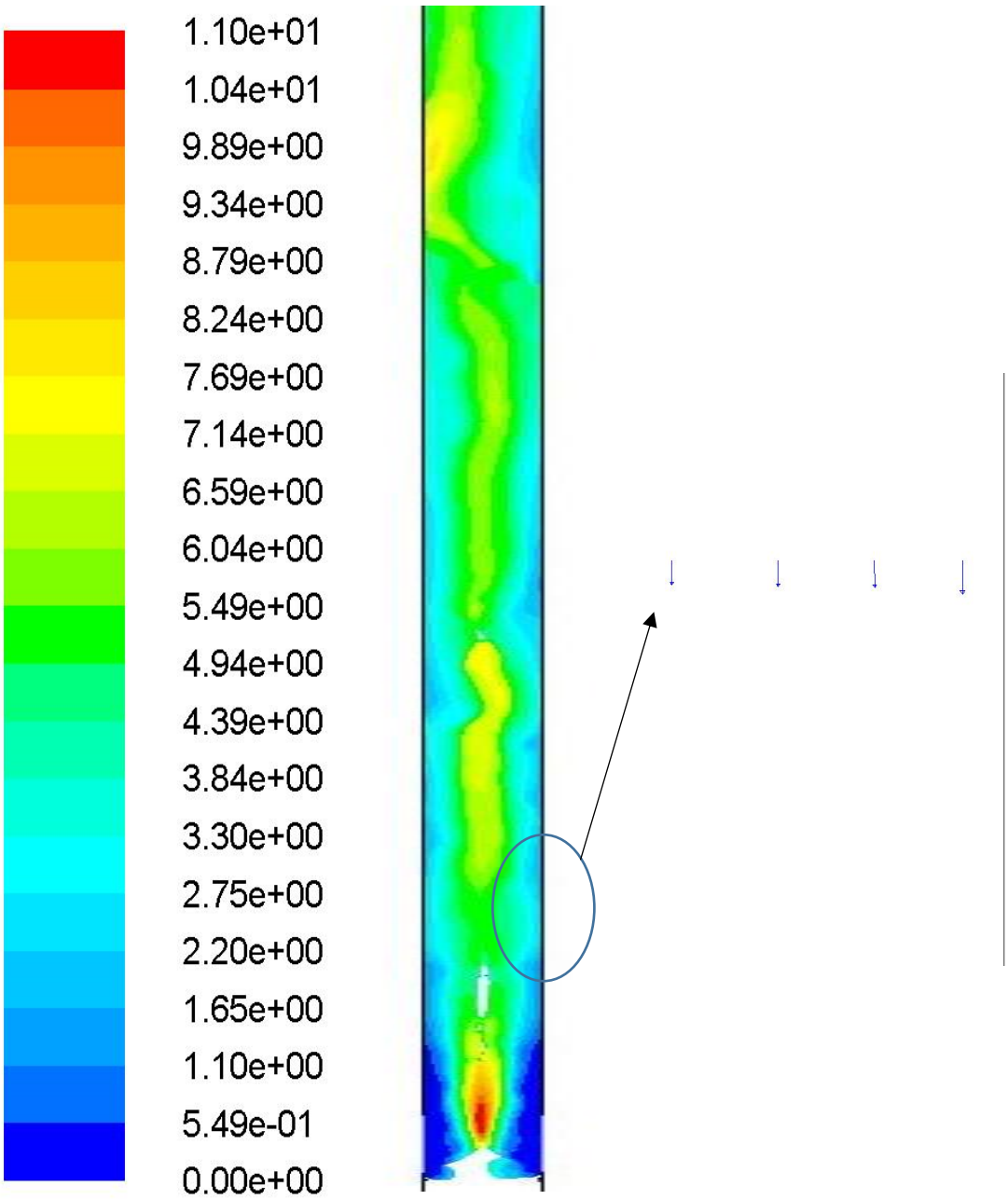

Fig. (24) Velocity Vector Near the Wall at 3 Sec using standard Wall Function

5.7 Volume Fraction of the solid phase at different times and shows the flow development:

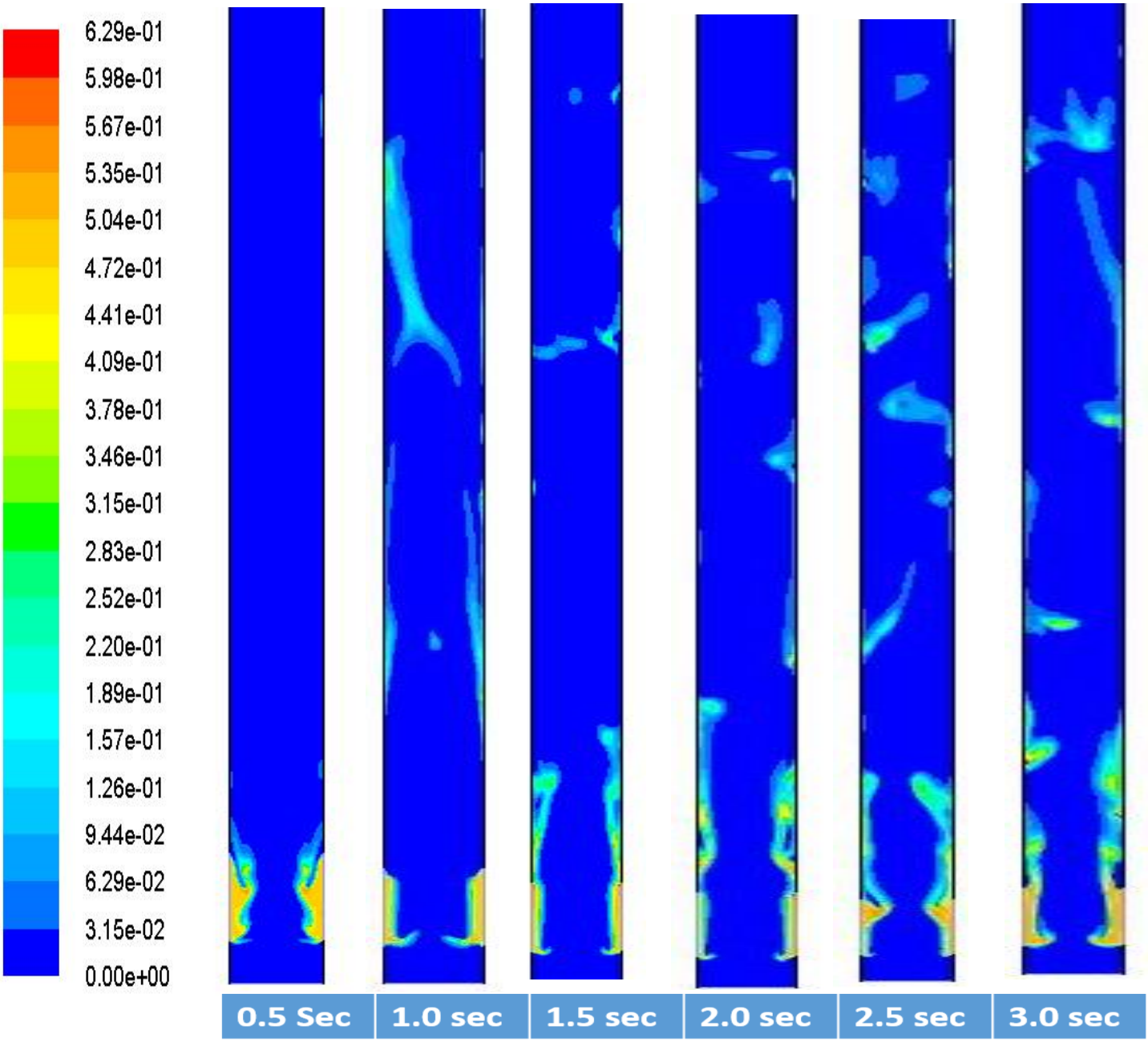

Fig. (25) Solid Particle Suspension using **Scalable Wall Function** at Different times

5.8 Volume Fraction of the solid phase at different times and shows the flow development:

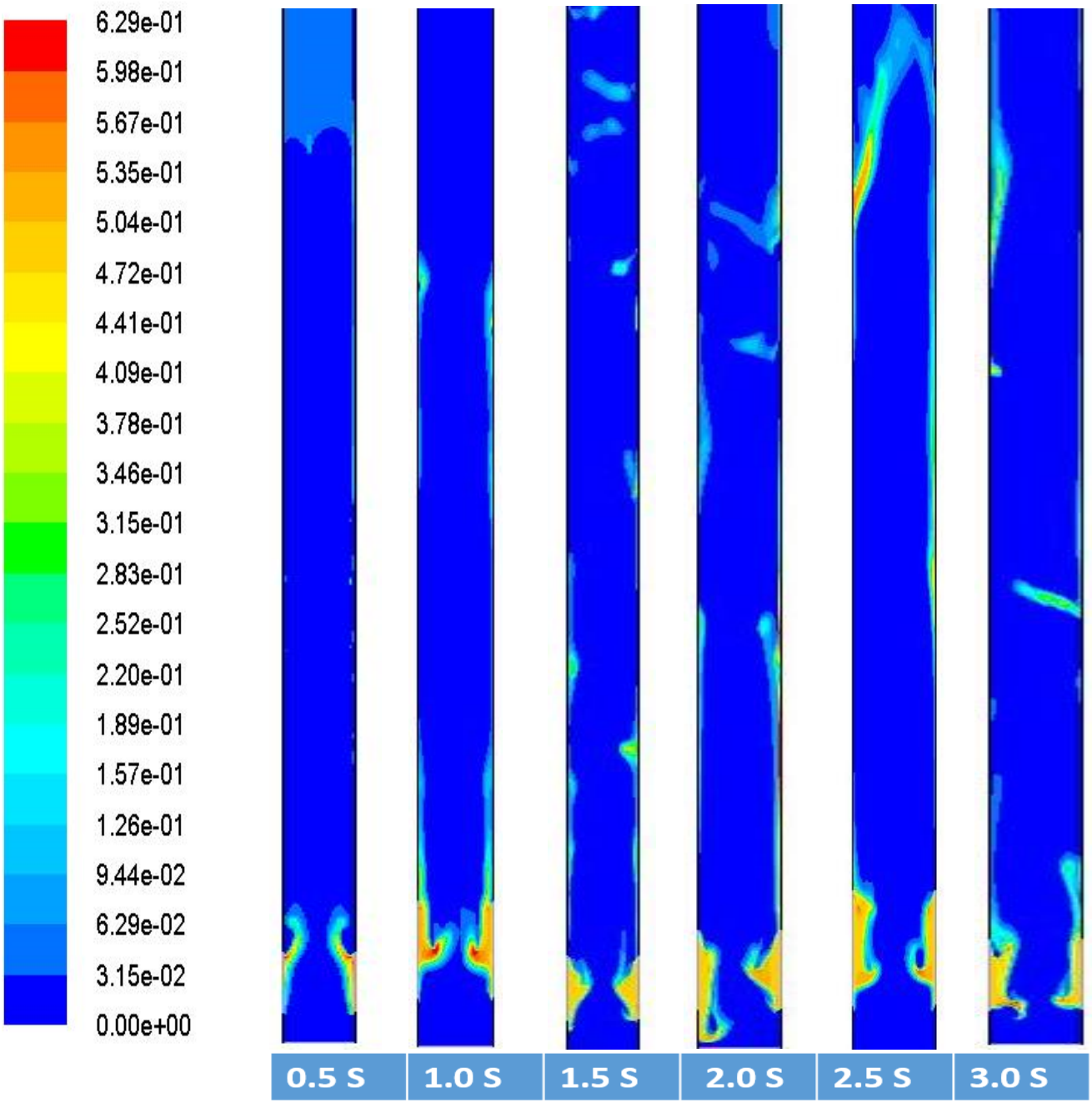

Fig. (26) Solid Particle Suspension using **Menter Lechner Wall Function** at Different times

6. References:

[1] Almuttahar, A.M.” CFD Modelling of the hydrodynamics of circulating Fluidized Bed Riser”, Master Thesis, UBC, 1997, pp. 7-20

[2] Gidaspow, Dimitri “Multiphase flow and Fluidization” Published by Boston: Academic Press. Edition-c1994. pp. 239-296

[3] Ansys Fluent Theory Guide, Release 2015, Ansys, Inc. pp 112-130

[4] Botao Peng (2009) “Study on Hydrodynamics Flow Mechanism in CFB Risers” PhD Thesis, University of Western Ontario

[5] Ansys User Guide, 2012, Ansys, Inc.